Northumbria Research Link

Journal Pre-proof

Intramuscular lipid concentration increased in localized regions of the lumbar muscles following 60-day bedrest

Enrico De Martino , Julie Hides , James M. Elliott ,
Mark A. Hoggarth , Jochen Zange , Kirsty Lindsay ,
Dorothée Debuse , Andrew Winnard , David Beard ,
Jonathan A Cook , Sauro E. Salomoni , Tobias Weber ,
Jonathan Scott , Paul W. Hodges , Nick Caplan

Please cite this article as: Enrico De Martino , Julie Hides , James M. Elliott , Mark A. Hoggarth , Jochen Zange , Kirsty Lindsay , Dorothée Debuse , Andrew Winnard , David Beard , Jonathan A Cook , Sauro E. Salomoni , Tobias Weber , Jonathan Scott , Paul W. Hodges , Nick Caplan , Intramuscular lipid concentration increased in localized regions of the lumbar muscles following 60-day bedrest, *The Spine Journal* (2021), doi: https://doi.org/10.1016/j.spinee.2021.11.007

Intramuscular lipid concentration increased in localized regions of the lumbar muscles following 60-day bedrest

Enrico De Martino[1], Julie Hides[2], James M. Elliott[3,4], Mark A. Hoggarth[3,5], Jochen Zange[6], Kirsty Lindsay[1], Dorothée Debuse[1], Andrew Winnard[1], David Beard[7], Jonathan A Cook[7,8], Sauro E. Salomoni[9], Tobias Weber[10,11], Jonathan Scott[10,11], Paul W. Hodges[9], Nick Caplan[1]

1. Aerospace Medicine and Rehabilitation Laboratory, Faculty of Health and Life Sciences, Northumbria University, Newcastle upon Tyne, United Kingdom
2. School of Health Sciences and Social Work, Griffith University, Nathan Campus, Brisbane, Australia
3. Northwestern University, Feinberg School of Medicine Department of Physical Therapy and Human Movement Sciences, Chicago, Illinois, USA
4. Northern Sydney Local Health District & The University of Sydney, Faculty of Medicine and Health, The Kolling Institute Sydney, Australia
5. Northwestern University, McCormick School of Engineering, Department of Biomedical Engineering, Evanston, Illinois, USA
6. Institute of Aerospace Medicine, German Aerospace Center (DLR), Cologne, Germany
7. NIHR Oxford Biomedical Research Centre, Nuffield Department of Orthopaedics, Rheumatology and Musculoskeletal Sciences, University of Oxford, Oxford, United Kingdom
8. Centre for Statistics in Medicine, Nuffield Department of Orthopaedics, Rheumatology and Musculoskeletal Sciences, University of Oxford, Oxford, United Kingdom
9. The University of Queensland, NHMRC Centre for Clinical Research Excellence in Spinal Pain, Injury and Health, School of Health and Rehabilitation Sciences, Brisbane, Australia
10. Space Medicine Team (HRE-OM), European Astronaut Centre, Cologne, Germany
11. KBR GmbH, Cologne, Germany

Corresponding author: Enrico De Martino

Faculty of Health and Life Sciences, Northumbria University

Newcastle upon Tyne, NE1 8ST, United Kingdom

Email: enrico.martino@northumbria.ac.uk

Conflict of interest: The authors declare that the research was conducted in the absence of any commercial or financial relationships that could be construed as a potential conflict of interest.

Highlights

- o Lipid accumulated in lumbar multifidus and erector spinae after bedrest
- o Lipid accumulation is distributed inhomogeneously in lumbar muscles after bedrest
- o Lipid accumulated more in medial/lateral than central region of lumbar multifidus
- o Inhomogeneous spatial lipid accumulation may influence lumbar spine function

Abstract

BACKGROUND CONTEXT: Prolonged bedrest induces accumulation of intramuscular lipid concentration (ILC) in the lumbar musculature; however, spatial distribution of ILC has not been determined. Artificial gravity (AG) mitigates some adaptations induced by 60-day bedrest by creating a head-to-feet force while participants are in a supine position.

PURPOSE: To quantify the spatial distribution of accumulation of ILC in the lumbar musculature after 60-day bedrest, and whether this can be mitigated by AG exposure.

STUDY DESIGN: Prospective longitudinal study.

PATIENT SAMPLE: Twenty-four healthy individuals (8 females) participated in the study: Eight received 30 min continuous AG (cAG); Eight received 6x5min AG (iAG), interspersed with rests; Eight were not exposed to AG (CRTL).

OUTCOME MEASURES: From 3T magnetic resonance imaging (MRI), axial images were selected to assess lumbar multifidus (LM), lumbar erector spinae (LES), quadratus lumborum (QL), and psoas major (PM) muscles from L1/L2 to L5/S1 intervertebral disc levels. Chemical shift-based 2-echo lipid/water Dixon sequence was used to measure tissue composition. Each lumbar muscle was segmented into four equal quartiles (from medial to lateral).

METHODS: Participants arrived at the facility for the baseline data collection before undergoing a 60-day strict 6° head-down tilt (HDT) bedrest period. MRI of the lumbopelvic region was conducted at baseline and Day-59 of bedrest. Participants performed all activities, including hygiene, in 6° HDT and were discouraged from moving excessively or unnecessarily.

RESULTS: At the L4/L5 and L5/S1 intervertebral disc levels, 60-day bedrest induced a greater increase in ILC in medial and lateral regions (~+4%) of the LM than central regions (~+2%; P<0.05). A smaller increase in ILC was induced in the lateral region of LES (~+1%) at L1/L2 and L2/L3 than at the centro-medial region (~+2%; P<0.05). There was no difference between CRTL and intervention groups.

CONCLUSIONS: Inhomogeneous spatial distribution of accumulation of ILC was found in the lumbar musculature after 60-day bedrest. These findings might reflect pathophysiological mechanisms related to muscle disuse and contribute to localized lumbar spine dysfunction. Altered spatial distribution of ILC may impair lumbar spine function after prolonged body unloading, which could increase injury risk to vulnerable soft tissues, such as the lumbar intervertebral discs. These novel results may represent a new biomarker of lumbar deconditioning for astronauts, bedridden, sedentary individuals, or those with chronic back pain. Changes are potentially modifiable but not by the AG protocols tested here.

Keywords: Short-arm centrifugation, Dixon sequence, Fatty infiltration, Adipose tissue, Magnetic resonance imaging, Lumbar multifidus, AGBRESA study, Space flight analog

Introduction

Movement and gravitational loading appear necessary to preserve spinal health. When vertical loading of the human body is reduced, such as experienced during prolonged bedrest or spaceflight, the lumbar spine undergoes rapid remodelling [1,2], which may increase the risk of low back pain or injury [3].

Although morphological changes of the lumbar spine (e.g., reduced muscle size, reduced lumbar lordosis) after prolonged vertical unloading have been extensively investigated [4–6], changes in muscle composition, such as intramuscular lipid concentration (ILC), have received less attention. Increased ILC has been reported in the lumbar multifidus (LM) muscle of individuals with persistent low back pain (LBP) [7–9], in adults with sway-back posture [10], elderly individuals [11–13], and astronauts after spaceflights [14]. Animal studies have shown time-dependent lipid accumulation after intervertebral disc injury [15,16], also supported by human data [17]. It has been proposed that the accumulation of intramuscular lipid may impact the capacity to meet functional demands to control the spine [15,17].

The spatial distribution of ILC in the LM and lumbar erector spinae (LES) muscles appears dependent on the vertebral level (greater accumulation at the lower lumbar vertebral levels [13,18,19]) and also on the muscle location, where the most medial regions, adjacent to the spinous processes, have proportionally greater ILC [13,20,21]. The spatial distribution of accumulation of ILC in lumbar musculature induced by prolonged disuse remains unclear. Investigation of such changes is necessary to guide the design of prevention and rehabilitation protocols. Importantly, as paraspinal muscles have a complex architectural anatomy [7,22,23] and because ILC has been shown to accumulate in the muscles of the lower lumbar spine [12,13,19], a detailed analysis of the muscles at all lumbar vertebral levels is necessary to understand any potential changes due to prolonged disuse.

Strict head-down tilt bedrest (HDTBR) have been used to investigate the effect of prolonged vertical unloading upon the human body [24]. This position unloads the body's upright weight [24], reduces energy requirements [25] and overall sensory stimulation [25]. In contrast, artificial gravity (AG), via centrifugation in a short-arm centrifuge, has been suggested to mitigate many of these effects by stimulating the proprioceptive, vestibular, and neuroendocrine systems [26,27]. As AG is associated with a large acceleration gradient along the body axes (~$1G_z$ at the lumbar vertebral level), it has also been proposed that a mechanical compressive force applied to the lumbar spine could stimulate the lumbar

4

muscles [28]. It is unknown whether the increased ILC in the lumbar musculature in response to exposure to prolonged HDTBR is homogeneous within the muscles and spinal levels or with spatial variation of accumulation, or whether this can be mitigated by exposure to AG. This study aimed to investigate the spatial distribution of lipid accumulation patterns in the lumbar musculature in response to HDTBR. Furthermore, we aimed to examine whether AG, either continuously or intermittent, could mitigate the localized increases in ILC.

Methods

Study Design

The study was conducted at the ":envihab" facility in Cologne (Germany) as part of the Artificial Gravity Bed Rest—European Space Agency (AGBRESA) study. Twenty-four healthy participants (16 males) were recruited and allocated to one of three groups: 1) Control (CTRL) group (N=8); 2) 30 minutes continuous AG (cAG) daily (N=8); 3) intermittent 6x5 minutes AG (iAG) daily (N=8). The sex, age, height, and weight of the participant groups were comparable (CRTL – 2 females, 34±8 years, 177±7 cm, 79±13 kg; cAG – 3 females, 32±10 years, 173±8 cm, 72±10 kg; iAG – 3 females, 34±11 years, 174±11 cm, 71±5 kg). The study size of 24 was selected based on previous HDTBR studies showing the protective effects of AG on bone resorption [29] and orthostatic tolerance [30]. Other measures from this study have been published elsewhere and showed that HDTBR induced increases in spinal length and area of lumbar intervertebral discs, a reduction in the lumbar lordosis, and atrophy of the LM, LES, and QL muscles [28].

The current study was performed in accordance with the International Guidelines for Standardization of bedrest in the spaceflight context [31]. The study consisted of a baseline data collection (BDC) period, followed by 60 days of strict 6° HDTBR period and 14-day rehabilitation [32]. Participants carried out all tasks, including hygiene, in a supine posture and were discouraged from making unnecessary movements [32]. They were allowed to lie supine or on their side but were advised to have at least one shoulder touching the bed at all times [33]. Participants received a controlled diet with a daily caloric intake of 1.3 times the metabolic rate at rest and were expected to eat all the food they were served [34]. The Ethics Committee of the Northern Rhine Medical Association approved this study (Düsseldorf, Germany, Application No. 2018143), and participants provided written informed consent to participate in the study. The study was registered at the German Clinical Trial Register under No. DKRS00015677.

Artificial gravity

Transfer to the centrifuge was accomplished with a specific tilt gurney, and participants were placed on the 3-meter centrifuge arm in supine position (6° head-down tilt). During centrifugation, participants were exposed to $1G_z$ at their estimated center of mass. They could perform anti-orthostatic maneuvers, such as heel raises and shallow knee bends, to avoid calf pain and maintain circulation while spinning but were otherwise instructed to remain still [33]. Continuous medical monitoring to ensure participant safety was implemented during all centrifuge runs [33].

MRI Measurements

MRIs were collected using a 3 Tesla Magnetom Vision system (Siemens, Erlangen, Germany). Participants were positioned in supine lying on the scanning table with their knees and hips supported in slight flexion by a pillow. MRIs were acquired two days before HDTBR (BDC) and on the 59th day of HDTBR (HDT59) and stored for offline analysis. A set of 64 transverse images were acquired from the T12 vertebra to the sacrum (T1 weighted Dixon sequence, total acquisition time=5 minutes; slice thickness=4 mm; distance factor=20%, TR=7.02 ms, TE1=2.46 ms, TE2=3.69 ms, flip angle=5 deg; field of view=400 mm x 400 mm at 1.0 mm x 1.0 mm pixel size). Images were obtained with the fat and water in-phase and out of phase; then, fat (F) and water images (W) were reconstructed. Regions of interest (ROI) were manually traced over the lumbar paravertebral muscles using a semi-automated Matlab-based program [13,35]. The custom built Matlab (Natick, MA, USA) program automatically divided the ROI into quarters of equal area from medial (Q1) to lateral (Q4) based on the pixel number (Figure 1) [13,21]. ILC was calculated as the ratio of pixel intensities from the F and W images:

$$ILC = \frac{F}{(W + F)} * 100$$

Bilateral ILC measurements of the LM, LES, QL, and PM muscles were extracted from each transverse MRI [13,21]. Four slices were identified for each of five lumbar intervertebral discs (L1/L2, L2/L3, L3/L4, L4/L5, L5/S1; Figure 1). The ILC measurements for the MRIs were averaged for the 4 slices at each lumbar region and the left- and right-side. The changes were calculated as a difference to the BDC (HDT59 value − BDC value) for each muscle quartile for the statistical analysis. Reliability of quantification of fat distribution in the lumbar paravertebral muscles in the transverse plane has been demonstrated in humans

6

[35]. This ILC evaluation technique has been validated in pig and rabbit models using the reference standard biopsy/histology [36].

Statistical analysis

Statistical analysis was undertaken using SPSS (Version 25, IBM, Chicago, USA). All results are presented as mean (standard deviation, SD). Statistical significance was set at the (2-sided) 0.05 level. Outcomes were assessed for normality using visual inspection (histograms and Q–Q plots) and Shapiro–Wilk tests. First, a two-way Analysis of Variance (ANOVA) was used to examine the distribution of ILC throughout the lumbar paraspinal muscles at BDC (before HDTBR) using Quartile (Q1, Q2, Q3, and Q4) and Level (L1/L2, L2/L3, L3/L4, L4/L5, and L5/S1) as within-group factors. Changes in response to HDTBR were assessed with three-way ANOVA using time (BDC and HDT59) and Quartile (Q1, Q2, Q3, and Q4) as repeated measures and Groups (iAG, cAG, CTRL) as between-group factors. Since the percentage of ILC in the quartiles was different in all muscles and all vertebral levels, a mixed-model ANOVA was used for change in ILC after HDTBR (HDT59 value − BDC value) between Groups (CRTL, cAG, iAG; between-group factor) and Quartile (Q1, Q2, Q3, and Q4; within-subject factor) to specifically investigate the spatial variation of lipid accumulation. The interaction effect of Group and Quartile was included in all models. The Greenhouse–Geisser approach was used to correct against violations of sphericity. Effect sizes (partial eta-squared: $\eta^2_{partial}$) were reported. Post hoc pairwise comparisons were performed using Bonferroni corrected multiple comparisons when significant main effect or interaction and corresponding 95% confidence intervals were generated.

Results

Intramuscular lipid concentration at BDC

Figure 1 shows the ILC patterns at BDC. For all paraspinal muscles, the 2-way ANOVA showed a main effect of Quartile (all − $F_{3,69} > 35$; $P < 0.001$) and Level*Quartile interaction (all − $F_{12,276} > 3.5$; $P < 0.05$), but the effect of Level was only found for LM and LES (both − $F_{4,92} > 40$; $P < 0.001$).

For the LM muscle, pairwise comparisons showed higher values in ILC at the L3/L4, L4/L5, and L5/S1 vertebral levels compared with L1/L2 and L2/L3 (all − $P < 0.01$), with the highest value at L5/S1 (all − $P < 0.01$). Except for L5/S1, the ILC progressively decreased from Q1 (medial) to Q3 (all − $P < 0.001$) and increased again from Q3 to Q4 (all − P <

7

0.001). This pattern slightly differed at the L5/S1 vertebral level, where the highest values were found in Q1, Q2 and Q4 compared with Q3 (all − P < 0.01).

For the LES muscle, pairwise comparisons showed a progressive increase in ILC from the L2/L3 to L5/S1 vertebral levels (all − P < 0.001), with the highest value at L5/S1 (all − P < 0.01). Except for L5/S1, the ILC progressively decreased from Q1 (medial) to Q4 (lateral) (all − P < 0.05). This pattern differed at the L5/S1vertebral level, where the highest values were found in Q1 and Q4 compared with Q2 and Q3 (all − P < 0.001).

For the PM muscle, the ILC was higher in Q1 (medial) compared with Q2, Q3, and Q4 (P < 0.05) for all vertebral levels except for L5/S1, where no difference in quartiles was found. For the QL muscle, ILC was higher in Q1 (medial) and Q4 (lateral) compared with Q2 and Q3 (all - P < 0.05) for L1/L2 and L3/L4 vertebral levels. This pattern slightly differed at L2/L3 vertebral level, where the highest values were found in Q1 compared with Q2, Q3, and Q4 (all - P < 0.05).

Intramuscular lipid concentration in LM muscle after HDTBR

The changes in ILC at each vertebral level are shown in Figure 2. At L4/L5 and L5/S1 vertebral levels, the three-way ANOVA showed a main effect of Time (F > 100; P < 0.001), Quartile (F > 25; P < 0.001), and Time*Quartile interaction (F > 5; P < 0.01). No significant main effect of Groups or other interactions were found (data and statistical analysis: Supplementary Table 1 and 2). Analysis of the change in ILC after HDTBR revealed a significant effect of Quartile at the L4/L5 ($F_{2.4,51.2}$ = 7.1; P = 0.001) and L5/S1 ($F_{2.0,42.2}$ = 5.7; P = 0.006) vertebral levels (Table 1 and Figure 3). At the level of the L4/L5, pairwise comparisons showed a greater increase in ILC in Q1 than Q3 (P = 0.044; CI 95% [0.40, 3.99]), Q2 than Q3 (P = 0.001; CI 95% [0.77, 3.10]) and Q4 than Q3 (P = 0.001; CI 95% [1.10, 4.88]). At the L5/S1 vertebral level, pairwise comparisons showed a greater increase in ILC in Q4 than Q2 (P = 0.007; CI 95% [0.80, 7.10]) and Q4 than Q3 (P = 0.017; CI 95% [0.07, 6.71]). There was no difference between Groups (main effect − $F_{2,21}$ < 2.5; P > 0.1) or interaction bewteen Quartile*Groups (all − $F_{3.6,38.0}$ < 1.5; P > 0.2).

At L1/L2, L2/L3 and L3/L4 vertebral levels, the three-way ANOVA showed a main effect of Time (F > 10; P < 0.005), Quartile (F > 25; P < 0.001). No significant main effect of Groups or other interactions were found (data and statistical analysis: Supplementary Table 1 and 2).

Intramuscular lipid concentration in LES muscle after HDTBR

At L1/L2 and L2/L3 vertebral levels, the three-way ANOVA showed a main effect of Time ($F > 30$; $P < 0.001$), Quartile ($F > 8$; $P < 0.001$), and Time*Quartile interaction ($F > 3$; $P < 0.05$). No significant main effect of Groups or other interactions were found (data and statistical analysis: Supplementary Table 3 and 4). Analysis of the change in ILC after HDTBR revealed a significant effect of Quartile at the levels of the L1/L2 ($F_{2.2,46.3} = 3.3$; $P = 0.042$) and L2/L3 ($F_{2.0,42.2} = 5.7$; $P = 0.006$) vertebral levels (Table 2 and Figure 4). At the L1/L2, there was a greater increased in ILC in Q4 than Q2 ($P = 0.04$; CI 95% [0.01, 2.88]). At the L2/L3 level, pairwise comparisons showed a greater increase in ILC in Q1 than Q4 ($P = 0.03$; CI 95% [0.06, 1.42]), Q2 than Q4 ($P = 0.01$; CI 95% [0.65 2.73]) and Q3 than Q4 ($P = 0.04$; CI 95% [0.02, 1.39]). There was no difference between Group (main effect – $F_{2,21} < 3$; $P > 0.05$) or interaction between Quartile*Groups (all – $F_{3.4,36.1} < 2.5$; $P > 0.05$).

At L3/L4, L4/L5 and L5/S1 vertebral levels, the three-way ANOVA showed a main effect of Time ($F > 15$; $P < 0.001$), Quartile ($F > 40$; $P < 0.001$), without any main effect of Groups or other interactions (data and statistical analysis: Supplementary Table 3 and 4).

Intramuscular lipid concentration in PM and QL muscles after HDTBR

At all vertebral levels, the three-way ANOVA showed a main effect of Quartile ($F > 8$; $P < 0.001$). No significant main effect of Time, Groups or other interactions were found (data and statistical analysis: Supplementary Table 5, 6, 7, and 8). Analysis of the change in ILC did not differ between Quartiles of PM or QL (Main effects – $F_{2.2,46.7} < 2.5$; $P > 0.05$). There was no difference between Groups (all – $F_{2,21} < 1$; $P > 0.05$) or interactions between Quartile*Groups (all – $F_{3.9,41.1} < 2$; $P > 0.05$) at any intervertebral disc level for these muscles (Table 3 and 4; Figure 5 and 6).

Discussion

This study identified and quantified the spatial pattern of accumulation of ILC in the lumbar musculature after 60-day HDTBR. Our results demonstrated a greater increase in lipid proportion in medial and lateral regions of the LM muscle at the L4/L5 and S1/L5 vertebral levels than in other regions and levels of the muscle. In contrast, a smaller increase in lipid proportions was observed in the lateral region of the LES muscle at the L1/L2 and L2/L3 vertebral levels than in other regions and levels of the muscle. No changes in lipid proportion

were detected in the PM and QL muscles after the HDTBR. Finally, exposure to AG did not change the accumulation of ILC.

Intramuscular lipid concentration in LM muscle

The current results showed that ILC increased in all LM muscle regions at all vertebral levels at the end of HDTBR compared with before. However, the lateral and medial regions and lower vertebral levels were most affected: At the L4/L5 vertebral level, more than 4% lipid accumulation was found in the centro-medial (Q1 and Q2) lateral (Q4) regions. At the L5/S1 vertebral level, ILC had increased by more than 5% in the lateral (Q4) and medial region (Q1) after HDTBR. This inhomogeneous accumulation of ILC may be related to the complex architectural structure and functional differentiation between regions of the LM muscle [37–39]. The LM fascicles originate from the spinous process and adjacent lamina of each lumbar vertebra, descend caudolaterally, over 2-4 vertebral levels, and attach to mamillary processes, the iliac crest, and the dorsal surface of the sacrum [22,40]. In the current study, the lateral region (Q4) at the L4/L5 and L5/S1 vertebral levels is likely to represent the distal portion of the longer fascicles originating from upper lumbar vertebrae (laminae of L1 and L2) and attaching to the L4 and L5 mamillary processes and the dorsal sacral surface [22]. These longer fascicles have a moment arm that can increase the lumbar lordosis and extend the lumbar spine, as their line of action falls behind the lumbar lordotic curve [41], and this is supported by electromyography (EMG) data [38,39]. As other EMG recordings have shown that the paraspinal extensor muscles are not active in reclined/lying positions [42], this may explain the ILC increase seen in the lateral, longer torque producing fibers in response to HDTBR.

The deeper portion of the centro-medial regions (Q1-Q2) at L4/L5 vertebral level would represent some of the shorter fascicles originating from the laminae of L3 and L4 and attaching to the mamillary processes of L5, the capsule of the zygapophyseal joints, and the dorsal surface of the sacrum [22]. The deeper, shorter fascicles are less able to generate torque than the more superficial, longer fascicles. Some studies suggest that the shorter fascicles have a higher percentage of Type 1 muscle fibers [43], indicating a propensity for low-level tonic activation. EMG investigations have demonstrated that the short deep fibers are less affected by the direction of applied force than the long fascicles in functional loading tasks [38]. Although the mechanisms are unclear, our results may indicate that this deep fiber region is differently impacted by unloading than the adjacent longer fascicles. However, it is also important to consider that ILC accumulates adjacent to the bone (spinous

process/lamina) and adjacent to the thick inter-muscular fascia (lateral aspect of muscle), as shown by our measurements before HDTBR, suggesting that these portions of the muscles may have greater potential to accumulate lipid.

The level-specific accumulation of fat might be explained by regional differentiation in loading. The lower vertebral levels have close proximity to the sacropelvic complex [37,44,45] and are exposed to greater mechanical stress than the upper lumbar levels [46]. Animal studies have demonstrated that high mechanical stress regulates the expression of transcriptional factors influencing cell differentiation [47]. Decreased cyclic mechanical stress leads to upregulation of adipogenic transcription factors [48] and reduced expression of factors that inhibit myoblast transdifferentiation to adipocytes [49]. Taken together with the results of the current study, we hypothesize that the muscle fibers at the lower vertebral levels, which are subjected to higher mechanical stress [46], might have a higher propensity to accumulate lipids when the lumbar spine is unloaded.

Intramuscular lipid concentration in LES muscle

Similar to the LM muscle, ILC in the LES muscle also tended to accumulate at the lowest lumbar vertebral levels, and a high percentage change in ILC with HDTBR was observed in medial and lateral regions at the L4/L5 and L5/S1 vertebral levels. Although still unknown, structural muscle changes close to these regions may have important biomechanical implications, as internal forces and moments produced by the muscles across those joints can be altered.

After HDTBR, lower intramuscular lipid accumulation was also found in the lateral region of LES muscle at the L1/L2 and L2/L3 vertebral levels (~ 1%) than in the centro-medial regions. The LES muscle consists of two large muscles: longissimus lumborum, medially, and iliocostalis lumborum, laterally [23,50]. At the L1 and L2 vertebral levels, the lateral division of the LES muscle contains many fibres that originate from the lumbar aponeurosis and insert on the 12-7th ribs (thoracic parts of iliocostalis lumborum muscle) [40]. Other functions of this lateral region of LES, such as a role in respiration, might lead to a lesser effect of HDTBR on this region. Although quiet breathing in supine does not involve activation of the abdominal and paraspinal muscles [51,52], inspiratory demand is increased in HDTBR as the diaphragm has to overcome the weight of the abdominal organs [53], and this has been suggested to explain the absence of major deconditioning of respiratory muscles after HDTBR [53]. Other functions such as a role in thoracolumbar rotation to move around the bed might also be involved.

11

Intramuscular lipid concentration in PM and QL muscles

In contrast to the LM and LES muscles, ILC in the PM and QL muscles did not accumulate at any vertebral levels and did not show any inhomogeneity of the spatial distribution of accumulation of ILC after HDTBR. Although the absence of ILC changes in the PM muscle is consistent with previous studies in astronauts [6,14], our results contrast with previous results showing an increase in the QL muscle after a 6-month spaceflight [6,14]. The absence of ILC accumulation in the current investigation may be explained by some essential distinctions between HDTBR and spaceflight. Microgravity is accompanied by the complete unloading of postural muscles, whereas these muscles still need to work against gravity during HDTBR, particularly when changing postures. For instance, our participants are likely to have recruited the QL muscle to laterally flex their spine during hygiene activities and when rolling onto their sides, dressing, and eating. Daily side-lying activities during the current HDTBR may have been sufficient to prevent the accumulation of ILC in the QL muscle. Alternatively, ILC accumulation in QL muscle may require long-lasting body unloading.

Clinical implications for patients and operational relevance for spaceflight

The present results expand previous findings indicating that higher adipose tissue accumulation in low back muscles is associated with physical inactivity [54]. Greater amounts of ILC in the LM muscle, rather than changes in muscle size, have been associated with an increased risk of high-intensity pain among adults with LBP [17]. Future studies should investigate whether reconditioning interventions following a period of prolonged unloading, such as HDTBR or spaceflight, can reverse the localized accumulation of ILC in the LM and LES muscles.

Space Agencies have renewed their focus on the Moon missions [55], and more astronauts are expected to go into space and work on the Moon in this decade. However, prolonged spaceflight may increase the risk of spinal injury, and optimal countermeasures to mitigate the deconditioning effect of mechanical unloading to the lumbar spine may be crucial. Our results showed that daily AG protocols did not significantly protect the muscles from these effects. Future studies should consider whether other paradigms are effective, such as prolonged AG exposure, higher compressive G_z, or the combination of AG with specific lumbar muscle exercises.

12

Limitations

The results of the current study should be interpreted in consideration of its limitations. Small sample sizes are a common limitation of HDTBR studies due to the intrinsically complex nature and expense of these studies. Nevertheless, similar HDT bed rest studies have included similar numbers of groups and participants and have found differences using the same statistical approach as the current study [56–58]. Because of the small sample size in the groups, only large effect sizes from countermeasures can be observed, and more subtle effects are likely to go unnoticed.

Although quartile segmentation has frequently been used to study ILC in cervical and lumbar muscles, this segmentation may be insufficient to detect more localized changes, and, due to the complex architecture of the muscles studied, future studies could consider a higher spatial resolution.

Conclusion

The current investigation suggests that ILC increased more in the medial and lateral regions than central regions of the lower LM muscle after 60-day HDTBR. In contrast, the LES muscle accumulated less ILC in the lateral than medio-central region of the upper lumbar spine. The present findings may represent a new target for lumbar muscle reconditioning for those exposed to prolonged extreme physical inactivity, astronauts, elderly, or individuals with chronic LBP.

References

[1]   Bailey JF, Miller SL, Khieu K, Neill CWO, Healey RM, Coughlin DG, et al. From the international space station to the clinic : how prolonged unloading may disrupt lumbar spine stability. Spine J 2018;18:7–14. https://doi.org/10.1016/j.spinee.2017.08.261.

[2]   Chang DG, Healey RM, Snyder AJ, Sayson J V., Macias BR, Coughlin DG, et al. Lumbar spine paraspinal muscle and intervertebral disc height changes in astronauts after long-duration spaceflight on the International Space Station. Spine (Phila Pa 1976) 2016;41:1917–24. https://doi.org/10.1097/BRS.0000000000001873.

[3]   Belavý DL, Adams M, Brisby H, Cagnie B, Danneels L, Fairbank J, et al. Disc herniations in astronauts: What causes them, and what does it tell us about herniation on earth? Eur Spine J 2016;25:144–54. https://doi.org/10.1007/s00586-015-3917-y.

[4]   Hides JA, Lambrecht G, Sexton CT, Pruett C, Petersen N, Jaekel P, et al. The effects of exposure to microgravity and reconditioning of the lumbar multifidus and anterolateral abdominal muscles: implications for people with LBP. Spine J 2020:1–14. https://doi.org/10.1016/j.spinee.2020.09.006.

[5]   Belavý DL, Armbrecht G, Richardson CA, Felsenberg D, Hides JA. Muscle atrophy and changes in spinal morphology: Is the lumbar spine vulnerable after prolonged bed-rest? Spine (Phila Pa 1976) 2011;36:137–45. https://doi.org/10.1097/BRS.0b013e3181cc93e8.

[6]   Burkhart K, Allaire B, Bouxsein ML. Negative Effects of Long-duration Spaceflight on Paraspinal Muscle Morphology. Spine (Phila Pa 1976) 2019;44:879–86. https://doi.org/10.1097/BRS.0000000002959.

[7]   Hodges PW, Danneels L. Changes in Structure and Function of the Back Muscles in Low Back Pain: Different Time Points, Observations, and Mechanisms. J Orthop Sport Phys Ther 2019;49:464–76. https://doi.org/10.2519/jospt.2019.8827.

[8]   Kjaer P, Bendix T, Sorensen JS, Korsholm L, Leboeuf-Yde C. Are MRI-defined fat infiltrations in the multifidus muscles associated with low back pain? BMC Med 2007;5:1–10. https://doi.org/10.1186/1741-7015-5-2.

[9]   Hildebrandt M, Fankhauser G, Meichtry A, Luomajoki H. Correlation between lumbar dysfunction and fat infiltration in lumbar multifidus muscles in patients with low back pain. BMC Musculoskelet Disord 2017:1–9. https://doi.org/10.1186/s12891-016-1376-1.

[10]   Pezolato A, De Vasconcelos EE, Defino HLA, Defino A, Nogueira-Barbosa MH. Fat infiltration in the lumbar multifidus and erector spinae muscles in subjects with sway-back posture. Eur Spine J 2012;21:2158–64. https://doi.org/10.1007/s00586-012-2286-z.

[11]   Dahlqvist JR, Vissing CR, Hedermann G, Thomsen C, Vissing J. Fat Replacement of Paraspinal Muscles with Aging in Healthy Adults. Med Sci Sports Exerc 2017;49:595–601. https://doi.org/10.1249/MSS.0000000000001119.

[12]   Crawford RJ, Filli L, Elliott JM, Nanz D, Fischer MA, Marcon M, et al. Age- and level-dependence of fatty infiltration in lumbar paravertebral muscles of healthy volunteers. Am J Neuroradiol 2015;37:742–8. https://doi.org/10.3174/ajnr.A4596.

[13]   Crawford RJ, Volken ÃT, Elliott J., Hoggarth MA, Dpt MS, Samartzis D. Geography

of Lumbar Paravertebral Muscle. Spine (Phila Pa 1976) 2019;44:1294–302. https://doi.org/10.1097/BRS.0000000000003060.

[14] McNamara KP, Greene KA, Moore AM, Lenchik L, Weaver AA. Lumbopelvic muscle changes following long-duration spaceflight. Front Physiol 2019;10. https://doi.org/10.3389/fphys.2019.00627.

[15] Hodges PW, James G, Blomster L, Hall L, Schmid A, Shu C, et al. Multifidus Muscle Changes after Back Injury Are Characterized by Structural Remodeling of Muscle, Adipose and Connective Tissue, but Not Muscle Atrophy: Molecular and Morphological Evidence. Spine (Phila Pa 1976) 2015;40:1057–71. https://doi.org/10.1097/BRS.0000000000000972.

[16] Hodges PW, James G, Blomster L, Hall L, Schmid AB, Shu C, et al. Can proinflammatory cytokine gene expression explain multifidus muscle fiber changes after an intervertebral disc lesion? Spine (Phila Pa 1976) 2014;39:1010–7. https://doi.org/10.1097/BRS.0000000000000318.

[17] Teichtahl AJ, Urquhart DM, Wang Y, Wluka AE, Wijethilake P, O'Sullivan R, et al. Fat infiltration of paraspinal muscles is associated with low back pain, disability, and structural abnormalities in community-based adults. Spine J 2015;15:1593–601. https://doi.org/10.1016/j.spinee.2015.03.039.

[18] Fortin M, Lazáry À, Varga PP, Battié MC. Association between paraspinal muscle morphology, clinical symptoms and functional status in patients with lumbar spinal stenosis. Eur Spine J 2017;26:2543–51. https://doi.org/10.1007/s00586-017-5228-y.

[19] Lee SH, Park SW, Kim YB, Nam TK, Lee YS. The fatty degeneration of lumbar paraspinal muscles on computed tomography scan according to age and disc level. Spine J 2017;17:81–7. https://doi.org/10.1016/j.spinee.2016.08.001.

[20] Smith AC, Albin SR, Abbott R, Crawford RJ, Hoggarth MA, Wasielewski M, et al. Confirming the geography of fatty infiltration in the deep cervical extensor muscles in whiplash recovery. Sci Rep 2020;10:1–8. https://doi.org/10.1038/s41598-020-68452-x.

[21] Abbott R, Peolsson A, West J, Elliott JM, Åslund U, Karlsson A, et al. The qualitative grading of muscle fat infiltration in whiplash using fat and water magnetic resonance imaging. Spine J 2018;18:717–25. https://doi.org/10.1016/j.spinee.2017.08.233.

[22] Macintosh JE, Valencia F, Bogduk N, Munro R. The morphology multifidus of the human lumbar. Clin Biomech 1986;1:196–204.

[23] Macintosh JE, Bogduk N. The morphology of the lumbar erector spinae. Spine (Phila Pa 1976) 1987;12:658–68.

[24] Hargens AR, Vico L. Long-duration bed rest as an analog to microgravity. J Appl Physiol 2016;120:891–903. https://doi.org/10.1152/japplphysiol.00935.2015.

[25] Pavy-Le Traon A, Heer M, Narici M V., Rittweger J, Vernikos J. From space to Earth: Advances in human physiology from 20 years of bed rest studies. Eur J Appl Physiol 2007;101:143–94. https://doi.org/10.1007/s00421-007-0474-z.

[26] Clément GR, Bukley AP, Paloski WH. Artificial gravity as a countermeasure for mitigating physiological deconditioning during long-duration space missions. Front Syst Neurosci 2015;9:1–11. https://doi.org/10.3389/fnsys.2015.00092.

[27] Kotovskaya AR. The problem of artificial gravity: The current state and prospects. Hum Physiol 2010;36:780–7. https://doi.org/10.1134/s0362119710070078.

[28] De Martino E, Hides J, Elliott JM, Hoggarth M, Zange J, Lindsay K, et al. Lumbar muscle atrophy and increased relative intramuscular lipid concentration are not mitigated by daily artificial gravity following 60-day head-down tilt bed rest. J Appl Physiol 2021. https://doi.org/https://doi.org/10.1152/japplphysiol.00990.2020.

[29] Rittweger J, Bareille MP, Clément G, Linnarsson D, Paloski WH, Wuyts F, et al. Short-arm centrifugation as a partially effective musculoskeletal countermeasure during 5-day head-down tilt bed rest—results from the BRAG1 study. Eur J Appl Physiol 2015;115:1233–44. https://doi.org/10.1007/s00421-015-3120-1.

[30] Linnarsson D, Hughson RL, Fraser KS, Clément G, Karlsson LL, Mulder E, et al. Effects of an artificial gravity countermeasure on orthostatic tolerance, blood volumes and aerobic power after short-term bed rest (BR-AG1). J Appl Physiol 2015;118:29–35. https://doi.org/10.1152/japplphysiol.00061.2014.

[31] Sundblad P, Orlov O, Larina I, Cromwell R. Guidelines for standardization of bed rest studies of bed rest studies. Int Acad Astronaut 2014;Internatio:1–70.

[32] Ganse B, Bosutti A, Drey M, Degens H. Sixty days of head-down tilt bed rest with or without artificial gravity do not affect the neuromuscular secretome. Exp Cell Res 2021;399.

[33] Frett T, Green DA, Mulder E, Noppe A, Arz M, Pustowalow W, et al. Tolerability of daily intermittent or continuous short-arm centrifugation during 60-day 6o head down bed rest (AGBRESA study). PLoS One 2020;15:1–11. https://doi.org/10.1371/journal.pone.0239228.

[34] Kramer A, Venegas-Carro M, Mulder E, Lee JK, Moreno-Villanueva M, Bürkle A, et al. Cardiorespiratory and Neuromuscular Demand of Daily Centrifugation: Results From the 60-Day AGBRESA Bed Rest Study. Front Physiol 2020;11:1–9. https://doi.org/10.3389/fphys.2020.562377.

[35] Mhuiris ÁN, Volken T, Elliott JM, Hoggarth M, Samartzis D, Crawford RJ. Reliability of quantifying the spatial distribution of fatty infiltration in lumbar paravertebral muscles using a new segmentation method for T1-weighted MRI. BMC Musculoskelet Disord 2016;17:1–7. https://doi.org/10.1186/s12891-016-1090-z.

[36] Smith AC, Parrish TB, Abbott R, Hoggarth MA, Mendoza K, Chen YF, et al. Muscle-fat MRI: 1.5 Tesla and 3.0 Tesla versus histology. Muscle and Nerve 2014;50:170–6. https://doi.org/10.1002/mus.24255.

[37] Macintosh JE, Bogduk N. The biomechanics of the lumbar multifidus. Clin Biomech 1986;1:205–13. https://doi.org/10.1016/0268-0033(86)90147-6.

[38] Moseley GL, Hons BP, Hodges PW, Gandevia SC. Deep and Superficial Fibers of the Lumbar Multifidus Muscle Are Differentially Active During Voluntary Arm Movements. Spine (Phila Pa 1976) 2002;27:29–36.

[39] Moseley GL, Hodges PW, Gandevia SC. External perturbation of the trunk in standing humans differentially activates components of the medial back muscles. J Physiol 2003;547:581–7. https://doi.org/10.1113/jphysiol.2002.024950.

[40] Kalimo H, Rantanen J, Viljanen T, Einola S. Lumbar muscles: Structure and function.

Ann Med 1989;21:353–9. https://doi.org/10.3109/07853898909149220.

[41]   Bogduk N, Macintosh JE, Pearcy MJ. A universal model of the lumbar back muscles in the upright position. Spine (Phila Pa 1976) 1992;17:897–913.

[42]   Andersson GBJ, Ortengren R, Nachemson A. Intradiskal pressure, intra-abdominal pressure and myoelectric back muscle activity related to posture and loading. Clin Orthop Relat Res 1977;No. 129:156–64. https://doi.org/10.1097/00003086-197711000-00018.

[43]   Sirca A, Kostevc V. The fibre type composition of thoracic and lumbar paravertebral muscles in man. J Anat 1985;141:131–7.

[44]   Aspden RM. Intra-abdominal pressure and its role in spinal mechanics. Clin Biomech 1987;2:168–74. https://doi.org/10.1016/0268-0033(87)90010-6.

[45]   Bartelink DL. The role of abdominal pressure in relieving the pressure on the lumbar intervertebral discs. J Bone Joint Surg Br 1957;39 B:718–25. https://doi.org/10.1302/0301-620x.39b4.718.

[46]   Shirazi-Adl A, Parnianpour M. Effect of changes in lordosis on mechanics of the lumbar spine-lumbar curvature in lifting. J Spinal Disord 1999;12:426–47.

[47]   Akimoto T, Ushida T, Miyaki S, Tateishi T, Fukubayashi T. Mechanical stretch is a down-regulatory signal for differentation of C2C12 myogenic cells. Mater Sci Eng C 2001;17:75–8. https://doi.org/10.1016/S0928-4931(01)00340-X.

[48]   Kook SH, Lee HJ, Chung WT, Hwang IH, Lee SA, Kim BS, et al. Cyclic mechanical stretch stimulates the proliferation of C2C12 myoblasts and inhibits their differentiation via prolonged activation of p38 MAPK. Mol Cells 2008;25:479–86.

[49]   Akimoto T, Ushida T, Miyaki S, Akaogi H, Tsuchiya K, Yan Z, et al. Mechanical stretch inhibits myoblast-to-adipocyte differentiation through Wnt signaling. Biochem Biophys Res Commun 2005;329:381–5. https://doi.org/10.1016/j.bbrc.2005.01.136.

[50]   Bogduk N. A reappraisal of the anatomy of the human lumbar erector spinae. J Anat 1980;131:525–40.

[51]   Campbell BYEJM, Green JH. The variations in intra-abdominal pressure and the activity of the abdominal muscles during breathing; a study in man. J Physiol 1953;122:282–90.

[52]   Shirley D, Hodges PW, Eriksson AEM, Gandevia SC. Spinal stiffness changes throughout the respiratory cycle. J Appl Physiol 2003;95:1467–75. https://doi.org/10.1152/japplphysiol.00939.2002.

[53]   Montmerle S, Spaak J, Linnarsson D. Lung function during and after prolonged head-down bed rest. J Appl Physiol 2002;92:75–83. https://doi.org/10.1152/jappl.2002.92.1.75.

[54]   Sions JM, Coyle PC, Velasco TO, Elliott JM, Hicks GE. Multifidi Muscle Characteristics and Physical Function Among Older Adults With and Without Chronic Low Back Pain. Arch Phys Med Rehabil 2017;98:51–7. https://doi.org/10.1016/j.apmr.2016.07.027.

[55]   Roadmap GE. Lunar surface exploration scenario update. Suppl August 2020 n.d.

[56]   Belavý DL, Armbrecht G, Gast U, Richardson CA, Hides JA, Felsenberg D. Countermeasures against lumbar spine deconditioning in prolonged bed rest : resistive exercise with and without whole body vibration. J Appl Physiol 2010;109:1801–11. https://doi.org/10.1152/japplphysiol.00707.2010.

[57]   Holguin N, Muir J, Rubin C, Judex S. Short applications of very low-magnitude vibrations attenuate expansion of the intervertebral disc during extended bed rest. Spine J 2009;9:470–7. https://doi.org/10.1016/j.spinee.2009.02.009.

[58]   De Martino E, Salomoni SE, Hodges PW, Hides J, Lindsay K, Debuse D, et al. Intermittent short-arm centrifugation is a partially effective countermeasure against upright balance deterioration following 60-day head-down tilt bed rest. J Appl Physiol 2021. https://doi.org/https://doi.org/10.1152/japplphysiol.00180.2021.

Figure Captions

Figure 1. Sagittal projection of the lumbar spine. B: Characteristic location of lumbar paraspinal muscles identified for the measurement on axial images at BDC (average values of 24 participants). ILC was automatically quartiled based on equal pixel numbers. The colour scale represents the percentage of fat infiltration (0-52%).
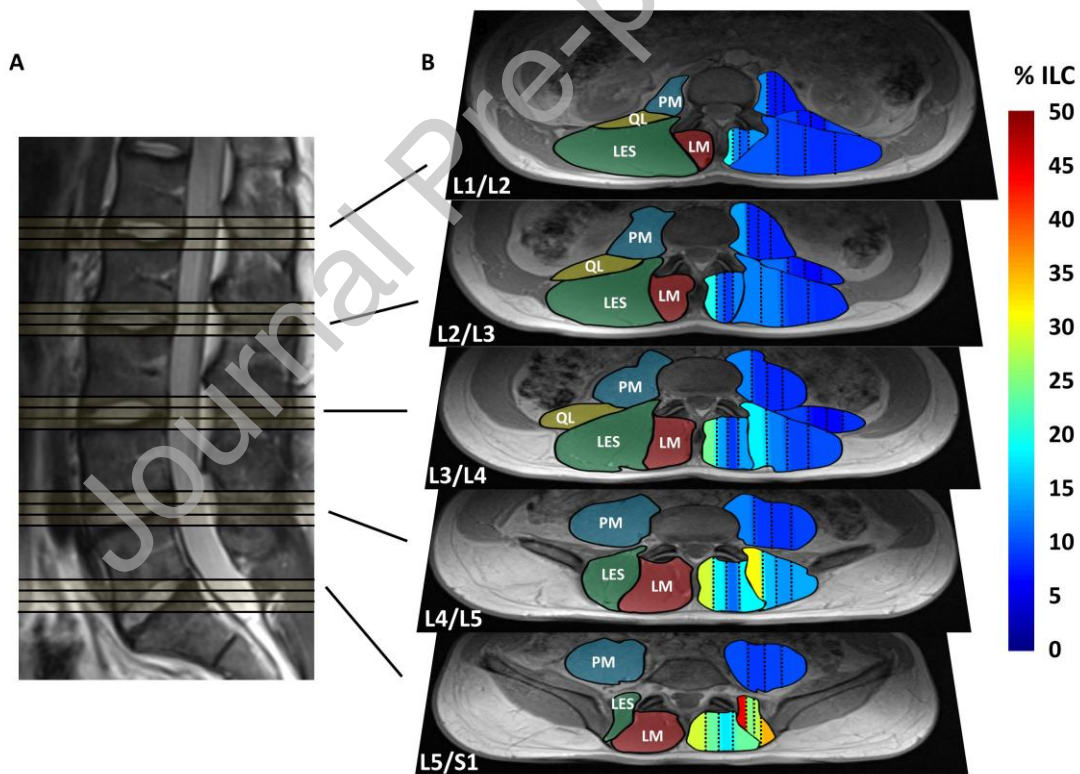
Figure 2. Absolute changes in ILC (HDT59-BDC). The colour scale represents delta ILC (from -2 to 8%). Note: Medial and lateral regions of LM accumulated more adipose tissue at the lower vertebral levels. Less adipose tissue accumulated in the lateral region of LES at the upper vertebral levels.
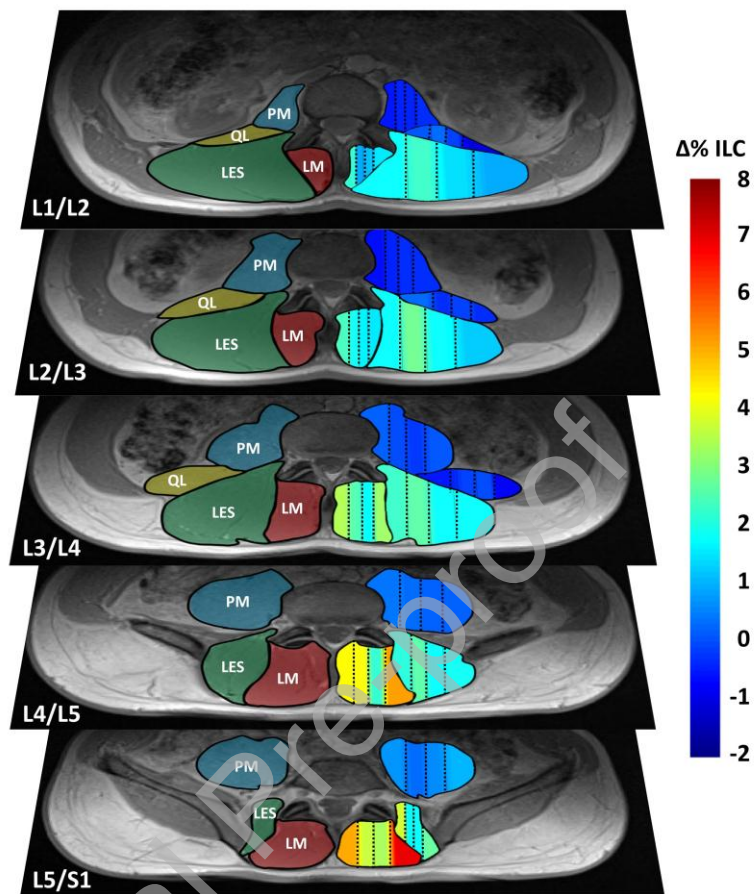
Figure 3. A) ILC of the lumbar multifidus muscle at BDC and HDT59 (average values of 24 participants) over quartiles (Q1 = medial; Q4 = lateral). B) Change in ILC after 60-days (HDT59 value – BDC value). * = Significant post hoc test within the Quartile (P<0.05).

21
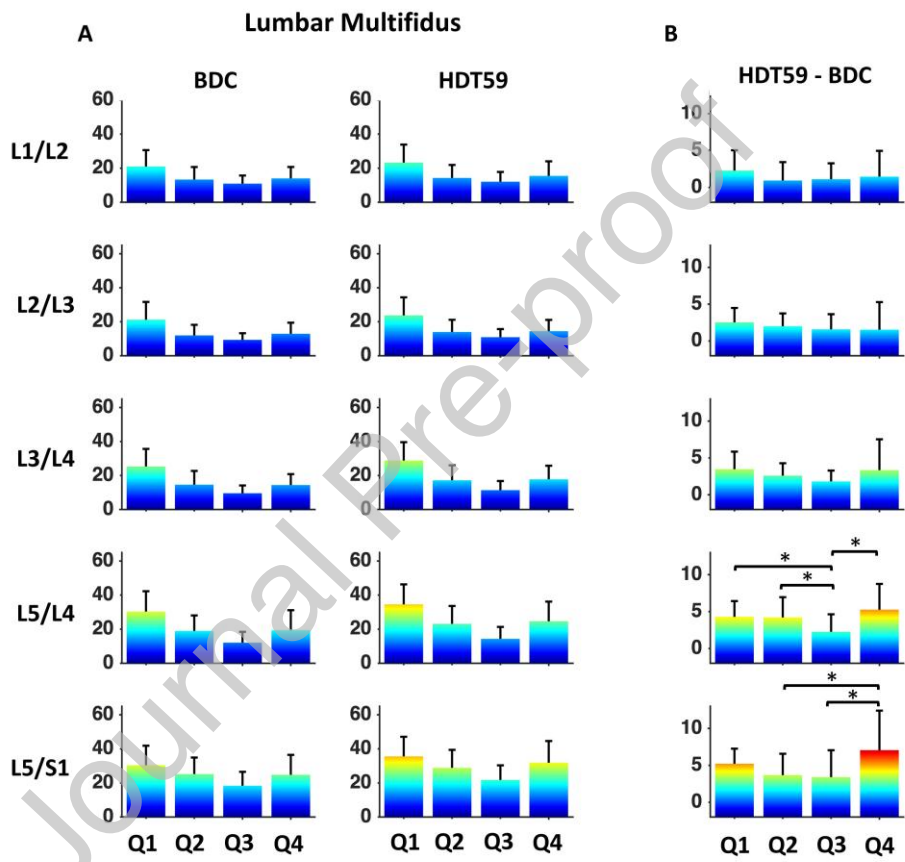
Figure 4. A) ILC of the lumbar erector spinae muscle at BDC and HDT59 (average values of 24 participants) over quartiles (Q1 = medial; Q4 = lateral). B) Change in ILC after 60-days (HDT59 value – BDC value). * = Significant post hoc test within the Quartile (P<0.05).
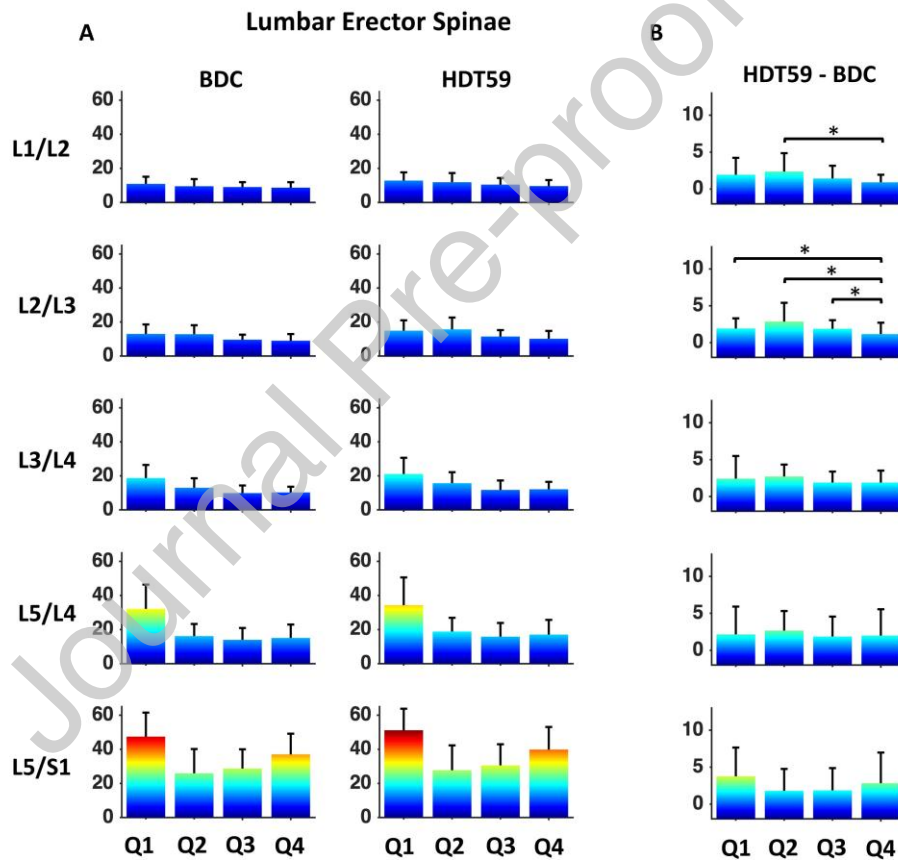
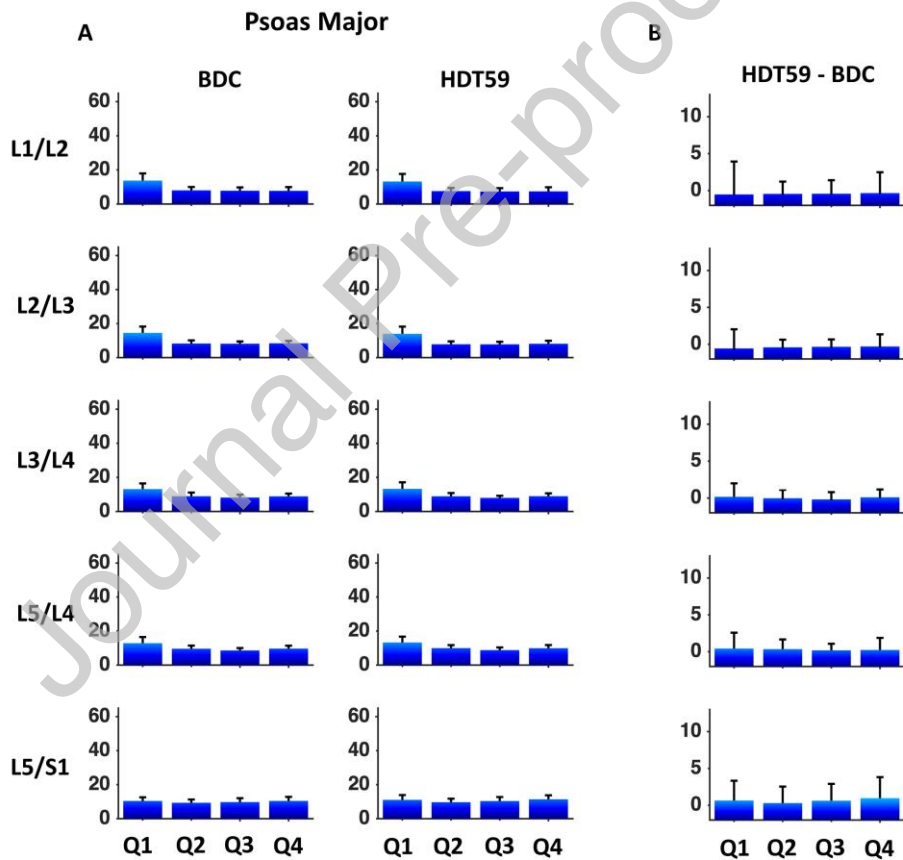**Figure 5** A) ILC of the psoas major muscle at BDC and HDT59 (average values of 24 participants) over quartiles (Q1 = medial; Q4 = lateral). B) Change in ILC after 60-days (HDT59 value – BDC value).

Figure 6. A) Intramuscular lipid concentration of the quadratus lumborum at BDC and HDT59 (average values of 24 participants) over quartiles (Q1 = medial; Q4 = lateral). B) Change in ILC after 60-days (HDT59 value − BDC value).
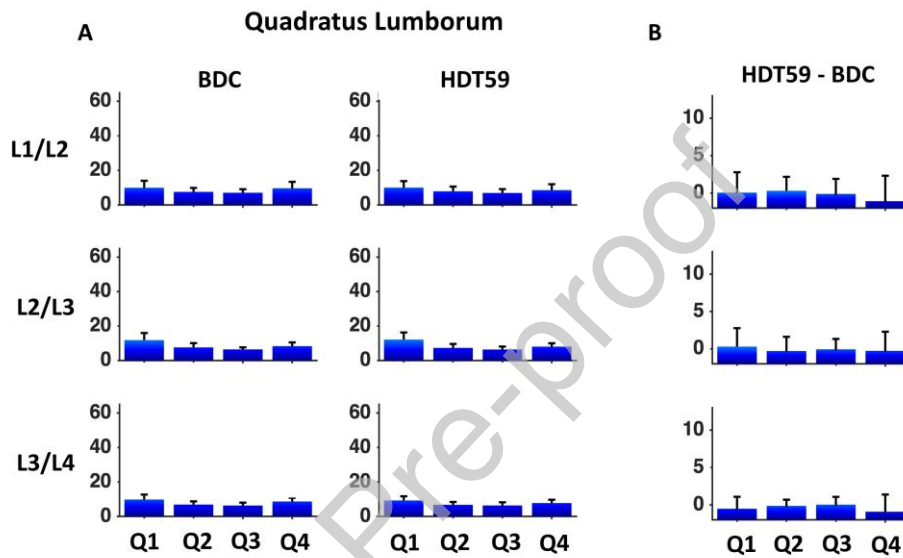
Table 1. Mean (± standard deviation) of lumbar multifidus change in ILC after HDTBR (HDT59 value − BDC value) from CTRL (N=8), cAG (N=8), and iAG (N=8). Q1 = medial; Q4 = lateral.

Lumbar multifidus								
Variable	Group	Quartile				Mixed model repeated measures ANOVA		
		Q1	Q2	Q3	Q4	Quartiles	Groups	Quartiles*Groups
L1/L2	CRTL	3.3±2.9	1.2±2.2	0.8±1.6	0.5±3.3	$F_{1.8, 38.0}=2.01$;	$F_{2, 21}=0.85$;	$F_{3.6, 38.0}=1.41$;

		Q1	Q2	Q3	Q4	Quartiles	Groups	Quartiles*Groups
intervertebral disc	cAG	2.5±2.3	1.9±2.8	2.1±2.3	2.0±2.8	P=0.122 $\eta^2_{partial}$=0.09	P=0.441 $\eta^2_{partial}$=0.75	P=0.224 $\eta^2_{partial}$=0.12
	iAG	1.0±2.8	0.2±2.1	0.5±2.4	1.9±4.4			
L2/L3 intervertebral disc	CRTL	2.2±2.9	2.2±2.2	1.1±1.7	1.1±3.9	$F_{1.8,39.4}$=1.26; P=0.297 $\eta^2_{partial}$=0.06	$F_{2,21}$=; P= $\eta^2_{partial}$=	$F_{3.7, 39.4}$=0.95; P=0.444 $\eta^2_{partial}$=0.08
	cAG	2.7±1.5	1.5±1.0	1.2±2.4	1.4±3.5			
	iAG	2.6±1.3	2.4±1.9	2.5±2.0	2.1±3.5			
L3/L4 intervertebral disc	CRTL	2.9±2.1	2.3±2.1	1.2±1.3	1.8±1.3	$F_{1.8,36.9}$=2.53; P=0.099 $\eta^2_{partial}$=0.11	$F_{2,21}$=2.42; P=0.113 $\eta^2_{partial}$=0.18	$F_{3.5,36.9}$=1.17; P=0.34 $\eta^2_{partial}$=0.10
	cAG	5.0±2.7	2.8±1.3	1.9±1.4	5.3±6.1			
	iAG	2.5±1.6	2.6±1.7	2.3±1.6	2.9±1.7			
L4/L5 intervertebral disc	CRTL	3.6±2.6	3.2±3.1	1.7±2.4	4.2±3.3	$F_{3,63}$=7.1; **P<0.001** $\eta^2_{partial}$=0.25	$F_{2,21}$=2.30; P=0.125 $\eta^2_{partial}$=0.18	$F_{6,63}$=1.08; P=0.38 $\eta^2_{partial}$=0.09
	cAG	5.6±1.7	4.4±2.6	2.2±2.7	6.5±3.7			
	iAG	3.7±1.5	4.9±2.7	2.9±2.2	5.0±2.8			
L5/S1 intervertebral disc	CRTL	4.5±1.8	4.2±3.3	3.9±3.6	6.4±4.9	$F_{2.0,42.2}$=5.74; **P=0.006** $\eta^2_{partial}$=0.22	$F_{2,21}$=0.32; P=0.729 $\eta^2_{partial}$=0.03	$F_{4.0,42.2}$=0.77; P=0.547 $\eta^2_{partial}$=0.07
	cAG	6.3±2.5	4.2±3.5	3.1±4.4	7.7±5.6			
	iAG	4.8±1.3	2.6±1.7	3.1±3.2	7.0±5.8			

Table 2. Mean (± standard deviation) of lumbar erector spinae change in ILC after HDTBR (HDT59 value − BDC value) from CTRL (N=8), cAG (N=8), and iAG (N=8). Q1 = medial; Q4 = lateral.

		Lumbar erector spinae						
Variable	Group	Quartile				Mixed model repeated measures ANOVA		
		Q1	Q2	Q3	Q4	Quartiles	Groups	Quartiles*Groups
L1/L2 intervertebral disc	CRTL	1.9±2.9	2.2±2.6	1.6±2.1	0.5±0.6	$F_{2.7,46.4}$=3.28; **P=0.032** $\eta^2_{partial}$=0.14	$F_{2,21}$=0.49; P=0.62 $\eta^2_{partial}$=0.04	$F_{4.4,46.4}$=0.18; P=0.982 $\eta^2_{partial}$=0.02
	cAG	2.4±1.6	2.9±2.9	1.5±1.9	1.3±1.1			
	iAG	1.5±2.4	2.0±2.1	1.2±1.3	0.8±1.2			
L2/L3 intervertebral disc	CRTL	2.1±1.3	3.2±2.6	1.8±1.5	1.4±1.5	$F_{1.9,41.2}$=9.82; **P<0.001** $\eta^2_{partial}$=0.32	$F_{2,21}$=0.54; P=0.594 $\eta^2_{partial}$=0.05	$F_{3.9,41.2}$=0.79; P=0.582 $\eta^2_{partial}$=0.07
	cAG	2.3±1.6	3.2±3.6	1.8±1.4	1.6±1.9			
	iAG	1.3±1.2	2.2±0.7	2.0±0.6	0.5±1.1			
L3/L4 intervertebral disc	CRTL	3.3±3.2	2.7±1.5	2.5±1.9	2.1±1.9	$F_{2.0,36.1}$=1.89; P=0.140 $\eta^2_{partial}$=0.08	$F_{2,21}$=0.62; P=0.548 $\eta^2_{partial}$=0.06	$F_{3.4,36.1}$=2.54; P=0.064 $\eta^2_{partial}$=0.19
	cAG	3.2±3.7	3.1±2.1	1.2±1.4	1.5±1.5			
	iAG	0.7±1.4	2.3±1.2	2.0±0.9	2.0±1.5			
L4/L5 intervertebral disc	CRTL	4.6±2.9	2.9±2.3	2.2±1.5	2.5±3.5	$F_{2.2,45.3}$=0.80; P=0.462 $\eta^2_{partial}$=0.04	$F_{2,21}$=2.84; P=0.081 $\eta^2_{partial}$=0.21	$F_{4.32,45.3}$=2.04; P=0.100 $\eta^2_{partial}$=0.16
	cAG	2.5±3.7	3.5±2.9	2.6±3.5	3.5±3.2			
	iAG	-0.6±3.1	1.5±2.6	0.8±2.7	0.1±3.5			
L5/S1 intervertebral disc	CRTL	4.4±3.7	2.2±2.1	2.0±1.6	3.5±2.9	$F_{2.1,43.1}$=1.80; P=0.156 $\eta^2_{partial}$=0.08	$F_{2,21}$=1.12; P=0.344 $\eta^2_{partial}$=0.09	$F_{4.1,43.1}$=1.79; P=0.951 $\eta^2_{partial}$=0.02
	cAG	3.8±4.5	2.2±3.7	3.1±4.2	2.8±4.7			
	iAG	3.1±3.9	0.9±3.0	0.4±2.3	2.1±4.9			

Table 3. Mean (± standard deviation) of psoas major change in ILC after HDTBR (HDT59 value − BDC value) from CTRL (N=8), cAG (N=8), and iAG (N=8). Q1 = medial; Q4 = lateral.

		Psoas Major						
Variable	Group	Quartile				Mixed model repeated measures ANOVA		
		Q1	Q2	Q3	Q4	Quartiles	Groups	Quartiles*Groups
L1/L2 interverte	CRTL	-1.5±0.6	-0.8±1.9	-1.5±1.9	-1.0±2.5	$F_{1.6,33.6}$=0.03; P=0.994	$F_{2,21}$=0.76; P=0.481	$F_{3.2,33.6}$=0.55; P=0.663
	cAG	-0.4±4.3	-0.3±1.8	0.6±1.9	0.8±3.9			

		Q1	Q2	Q3	Q4			
bral disc	iAG	0.3±2.9	0.2±1.3	-0.4±1.1	-0.8±1.6	$\eta^2_{partial}$=0.01	$\eta^2_{partial}$=0.07	$\eta^2_{partial}$=0.05
L2/L3 interverte bral disc	CRTL	-1.0±3.1	-0.7±1.1	0.7±1.2	-0.2±1.5	$F_{1.7,36.0}$=0.14; P=0.838	$F_{2,21}$=1.03; P=0.373	$F_{3.4,36.0}$=0.25; P=0.881
	cAG	0.9±2.1	-0.7±0.7	-0.3±0.9	-0.6±2.1			
	iAG	0.1±2.7	0.2±1.0	-0.0±0.8	-0.1±1.4	$\eta^2_{partial}$=0.01	$\eta^2_{partial}$=0.09	$\eta^2_{partial}$=0.02
L3/L4 interverte bral disc	CRTL	0.1±1.7	-0.3±1.5	-0.2±1.3	0.08±1.1	$F_{1.9,41.1}$=0.52; P=0.670	$F_{2,21}$=0.09; P=0.911	$F_{3.9,41.1}$=1.17; P=0.337
	cAG	-0.2±1.6	0.4±0.8	-0.3±0.8	0.6±0.7			
	iAG	0.6±2.2	-0.2±0.7	-0.1±0.9	-0.4±1.2	$\eta^2_{partial}$=0.03	$\eta^2_{partial}$=0.01	$\eta^2_{partial}$=0.10
L4/L5 interverte bral disc	CRTL	0.7±2.3	-0.1±1.4	-0.1±0.9	0.0±2.2	$F_{1.7,35.8}$=0.12; P=0.854	$F_{2,21}$=1.12; P=0.344	$F_{3.8,35.8}$=0.41; P=0.770
	cAG	0.0±2.2	0.8±1.0	0.2±1.2	0.4±1.6			
	iAG	0.5±2.2	0.3±1.5	0.4±0.3	0.3±1.2	$\eta^2_{partial}$=0.01	$\eta^2_{partial}$=0.09	$\eta^2_{partial}$=0.04
L5/S1 interverte bral disc	CRTL	-0.2±1.9	-0.7±1.3	-0.2±1.1	-0.3±2.0	$F_{1.8,39.4}$=1.02; P=0.390	$F_{2,21}$=1.14; P=0.340	$F_{3.8,39.4}$=0.47; P=0.745
	cAG	0.8±2.7	0.8±1.8	1.0±2.4	2.0±2.9			
	iAG	1.3±3.3	0.8±3.1	1.0±3.0	1.2±3.4	$\eta^2_{partial}$=0.05	$\eta^2_{partial}$=0.09	$\eta^2_{partial}$=0.04

Table 4. Mean (± standard deviation) of quadratus lumborum change in ILC after HDTBR (HDT59 value – BDC value) from CTRL (N=8), cAG (N=8), and iAG (N=8). Q1 = medial; Q4 = lateral.

Quadratus lumborum (%)								
Variable	Group	Quartile				Mixed model repeated measures ANOVA		
		Q1	Q2	Q3	Q4	Quartiles	Groups	Quartiles*Groups
L3/L4 intervertebral disc	CRTL	-0.9±2.1	0.2±2.8	0.5±2.9	-0.4±4.0	$F_{1.7,37.3}$=1.85; P=0.148	$F_{2,21}$=0.36; P=0.698	$F_{3.6,37.3}$=1.02; P=0.403
	cAG	0.6±2.6	0.1±1.0	-0.7±2.9	-2.3±2.9			
	iAG	0.5±3.4	0.7±1.6	-0.1±1.1	-0.5±3.1	$\eta^2_{partial}$=0.08	$\eta^2_{partial}$=0.03	$\eta^2_{partial}$=0.09
L4/L5 intervertebral disc	CRTL	-0.9±3.3	0.0±2.9	0.6±1.8	0.0±3.0	$F_{2.1,43.5}$=0.67; P=0.518	$F_{2,21}$=0.18; P=0.836	$F_{4.1,43.5}$=2.27; P=0.075
	cAG	0.6±2.1	-0.3±1.3	-0.4±1.2	-1.2±2.1			
	iAG	1.2±1.4	-0.5±1.3	-0.4±1.0	0.0±3.0	$\eta^2_{partial}$=0.03	$\eta^2_{partial}$=0.02	$\eta^2_{partial}$=0.18
L5/S1 intervertebral disc	CRTL	-1.2±2.0	-0.3±0.9	-0.2±1.1	-1.2±1.9	$F_{2.2,46.7}$=2.29; P=0.107	$F_{2,21}$=0.64; P=0.539	$F_{4.4,46.7}$=0.64; P=0.655
	cAG	-0.4±1.6	-0.0±0.7	0.2±1.2	-0.1±1.4			
	iAG	-0.3±1.8	-0.1±0.9	0.1±0.8	-1.6±3.2	$\eta^2_{partial}$=0.10	$\eta^2_{partial}$=0.06	$\eta^2_{partial}$=0.06

27